JOURNAL OF SOLID STATE CHEMISTRY 11, 135–147 (1974)

The Distribution of Nickel Ions among Octahedral and Tetrahedral Sites in $NiAl_2O_4$–$MgAl_2O_4$ Solid Solutions

P. PORTA*

Centro di Studio (C.N.R.) su Struttura ed Attività Catalitica di Sistemi di Ossidi, Istituto di Chimica, Università di Roma, Roma, Italy

AND

F. S. STONE† AND R. G. TURNER

Department of Physical Chemistry, School of Chemistry, University of Bristol, Bristol BS8 1TS, England

Received December 14, 1973

The cation distribution in $NiAl_2O_4$ and in the solid solutions $Ni_xMg_{1-x}Al_2O_4$ with x ranging from 0.01 to 0.55 has been studied by X-ray analysis, magnetic susceptibility and reflectance spectroscopy.

The relative X-ray intensities of various reflections for each compound were measured and compared with intensities calculated for various models of cation distribution. Lattice parameters, magnetic moments of Ni^{2+}, and the position of nickel absorption bands have also been measured. The results show that all specimens have a predominantly octahedral distribution for their nickel ions, and that there is a small change towards a random distribution when the quenching temperature is increased from 1273 to 1673°K.

Both X-ray and magnetic results show that the fraction, α, of Ni^{2+} ions on tetrahedral sites varies with nickel content. For samples quenched from 1273°K, $NiAl_2O_4$ is 78% inverse, but between $x = 1.0$ and $x = 0.25$ the value of α decreases from 0.22 towards 0.1. Thus, the fraction of nickel on octahedral sites in the solid solutions is higher than in $NiAl_2O_4$. The effect is linked with an increase in Dq for the Ni^{2+} ion. Below $x = 0.25$, there is tentative evidence that α may increase. In nickel-dilute solutions the matrix as a whole is nearly normal, and it is suggested that Madelung energy may then be more effective in counteracting the octahedral stabilization of nickel. The same trend is observed in the specimens quenched from 1673°K.

Introduction

The spinel structure affords a particularly good opportunity to explore the relative stabilities of ions in octahedral and tetrahedral coordination. For a binary oxidic spinel containing divalent, X, and trivalent, Y, cations, two extreme distributions of cations among the available sites are possible: the "normal" $X[Y_2]O_4$ and the "inverse" distribution $Y[XY]O_4$ (*1*), where the ions in the octahedral sites are written between square brackets. These arrangements, however, are limiting cases (*2*); intermediate distributions, such as the particular "random" or "statistical" distribution $X_{1/3}Y_{2/3}[X_{2/3}Y_{4/3}]O_4$, are also known. In the most general case it is convenient to characterize the cation distribution by the general formula $X_{1-2\lambda}Y_{2\lambda}[X_{2\lambda}Y_{2-2\lambda}]O_4$, where λ is the fraction of the Y trivalent cations on the tetrahedral sites

* Present address: Istituto di Chimica Inorganica, Università di Roma, 00185-Roma, Italy.

† Present address: School of Chemistry and Chemical Engineering, University of Bath, Bath BA2 7AY, England.

and equals zero, 0.5 and 1/3 for normal, inverse and random distribution, respectively.

The distribution of cations among the sites in spinels has been experimentally proved to be an equilibrium function of temperature, pressure and composition (*3*, *4*). The cation distribution which results in any given case is the result of a fine balance of the respective octahedral and tetrahedral preferences of the ions concerned. Certain factors which contribute to the octahedral and tetrahedral preferences of cations, such as the effects of ionic charge and ionic radius (*5*), are well known. There are other factors, however, such as crystal and ligand field effects (*6–8*), and anion polarization (*9*), about which much remains to be learnt. By making use of the property of solid solution formation, which is widespread in the spinel structure, gradual changes in the solid state chemistry can be effected simply by varying the composition of the solution (*10*). A knowledge of the influence of such compositional changes on cation distribution is of considerable interest for the further development of theoretical ideas.

The problem of determining the cation distribution in spinel solid solutions, however, is quite difficult, as there are now *three* cations to consider. For systems where two of the cations have similar X-ray scattering properties, but where one is a transition metal ion, magnetic and spectroscopic investigations can be used to supplement the conventional X-ray methods. In this paper we illustrate the combination of the three techniques to evaluate the nickel ion distribution in $Ni_xMg_{1-x}Al_2O_4$ and its dependence on nickel content.

$Ni_xMg_{1-x}Al_2O_4$ is of interest because of the rather similar preferences of Ni^{2+}, Mg^{2+} and Al^{3+} for octahedral coordination. This makes it an attractive choice in which to look for variations in the partition of individual cations with composition. The role of the magnetic and spectroscopic techniques is especially relevant because of the similar X-ray scattering powers of Mg^{2+} and Al^{3+} ions.

Experimental Procedure

Specimen Preparation and Analysis

Pure $NiAl_2O_4$, pure $MgAl_2O_4$ and 6 $Ni_xMg_{1-x}Al_2O_4$ solid solutions with x varying from 0.01 to 0.55 have been investigated. The starting materials were "Specpure" MgO and NiO supplied by Messrs. Johnson and Matthey, London and a pure grade of Al_2O_3 kindly provided by special request from Laporte Industries Ltd., Widnes. To prepare the spinels, the appropriate amounts of the component oxides were mixed into a paste

TABLE I

LIST OF $Ni_xMg_{1-x}Al_2O_4$ SPECIMENS WITH EXPERIMENTAL NICKEL CONTENTS x_{exp}, LATTICE PARAMETERS a (IN Å) AND MAGNETIC MOMENTS μ (IN μ_B)

		1673°K			1273°K		
Designation	x_{exp}	a	Δa^a	μ^b	a	Δa^a	μ^b
Ni–0	—	8.0835	—	—	8.0832	—	—
Ni–1	0.011	8.0832	0.0001	3.2	8.0828	0.0000	3.2
Ni–3	0.035	8.0827	0.0003	3.1	8.0820	0.0000	3.1
Ni–6	0.070	8.0817	0.0004	3.1	8.0810	0.0003	3.1
Ni–10	0.102	8.0809	0.0007	3.27	8.0797	0.0001	3.23
Ni–25	0.269	8.0758	0.0009	3.21	8.0747	0.0010	3.18
Ni–50	0.555	8.0665	0.0008	3.22	8.0655	0.0019	3.21
Ni–100	1.000	8.0514	—	3.27	8.0478	—	3.24

[a] Extents to which the lattice parameters for solid solutions lie above the line joining the a values of $MgAl_2O_4$ and $NiAl_2O_4$ (in Å).

[b] The values of μ for the Ni–1, Ni–3 and Ni–6 specimens are very approximate (see text).

with a small amount of water, dried, pelleted, and fired in air at 1673°K for 100 hr. For each composition, one batch of pellets was directly quenched in water from 1673°K, and a second batch was cooled to 1273°K, kept at this temperature for 50 hr and finally quenched in water from 1273°K.

Although nominal nickel contents could be specified from the weights of nickel oxide, magnesium oxide and alumina originally taken, it was considered desirable to analyse the spinels obtained for actual nickel content. The procedure adopted was to fuse a small sample with $KHSO_4$ in a platinum crucible, dissolve the cooled melt in dilute HCl and then filter. After the addition of tartaric acid to complex the aluminium, the solution was neutralized with ammonia and finally nickel was precipitated for gravimetric analysis by adding dimethylglyoxime. Two independent analyses, which gave reproducibility within 2%, were made on each spinel and the averaged results are given in Table I.

X-ray Investigations and Calculations of Intensities

Nickel-filtered Cu$K\alpha$ radiation was used to investigate all the compounds both for the lattice parameters and for the intensity measurements. For all specimens, X-ray diffraction patterns showed no lines other than those belonging to the cubic spinel structure. For precise determination of lattice constants a Philips camera (114.6 mm diam) with the asymmetric Straumanis film mounting method was used. For all specimens the reflections were very sharp. The following reflections in the region of $\theta = 60$–$90°$ were read by means of a Norelco measuring device with an accuracy of ±0.005 cm: 911, 664, 931, 844, 933, 10 2 0, 951, and 10 2 2. The corresponding lattice constants were then plotted for all samples against the Nelson–Riley function and the values of a were obtained by extrapolation to $\theta = 90°$. During the exposure (about 6 hr) the camera temperature was observed to vary within only 1–2°K. All lattice parameters extrapolated to $\theta = 90°$ were finally corrected for the thermal expansion coefficient (*11*) and the values of a reported in Table I are thus referred to 294°K. The error on a is 2×10^{-4} Å.

The relative integrated intensities of the 220, 311, 400, and 422 reflections were measured by pulse counting with a Philips high angle goniometer spectrometer using a flat-plate sample holder and a scanning rate of $2\theta = 0.25°$/min. All specimens were run twice and after correcting for background a mean value of the intensity was taken. The I_{400}/I_{220}, I_{311}/I_{220}, I_{400}/I_{422}, and I_{311}/I_{422} observed intensity ratios are given in Table II.

According to Bertaut (*12*) and to Weil, Bertaut, and Bochirol (*13*) the best information on cation distribution in spinels is achieved when comparing experimental and theoretical intensity ratios for reflections whose intensities (*i*) are independent (or very slightly dependent)

TABLE II

X-RAY DIFFRACTION INTENSITY RATIOS FROM THE EXPERIMENTALLY DETERMINED INTENSITIES OF THE REFLECTIONS 220, 311, 400, AND 422

Spinel	I_{400}/I_{220}		I_{311}/I_{220}		I_{400}/I_{422}		I_{311}/I_{422}	
	1673°K	1273°K	1673°K	1273°K	1673°K	1273°K	1673°K	1273°K
$MgAl_2O_4$	1.70	1.70	2.97	3.09	6.13	5.89	10.6	10.7
Ni-1	1.80	1.71	3.11	3.10	6.25	5.91	10.7	10.6
Ni-3	1.78	1.76	3.08	3.05	6.24	6.20	10.7	10.9
Ni-6	1.78	1.80	3.11	3.17	5.99	6.14	10.7	10.9
Ni-10	1.83	1.81	3.19	3.24	6.27	6.25	11.1	11.1
Ni-25	1.86	1.88	3.56	3.64	6.22	6.16	12.0	11.9
Ni-50	1.89	2.00	4.00	4.09	5.89	6.48	12.2	13.4
$NiAl_2O_4$	1.69	1.70	4.30	4.14	5.34	5.56	13.6	13.1

on the oxygen parameter u, (*ii*) vary with the inversion parameter in the opposite sense and (*iii*) do not differ strongly. The above reflections and ratios were selected because they most nearly meet these requirements. For $Ni_xMg_{1-x}Al_2O_4$, however, the (422) reflection is relatively weak and does not satisfactorily meet requirement (*iii*).

To determine the cation distribution and its variation, if any, with the composition x it is then necessary to calculate for each composition the above mentioned intensity ratios expected for given arrangements of the cations and compare them with the experimental values. For the calculation of the relative integrated intensity, I, of a given diffraction line from powder specimens, as observed in a diffractometer with a flat-plate sample holder, the following formula is valid (*14*):

$$I_{hkl} = |F|^2_{hkl} \cdot P \cdot L_p \qquad (1)$$

where F = structure factor, P = multiplicity factor, Lp = Lorentz-polarization factor.

It should be added that the calculated integrated intensities are valid at 0°K. Since the observed values are obtained at room temperature a suitable correction to Eq. (1) is in principle necessary for precise comparison. Since the spinels are high-melting compounds, the thermal vibration of the atoms at room temperature should not differ greatly from that at absolute zero, and this has been confirmed by Datta and Roy (*3a*) for $NiAl_2O_4$ and other spinels. Hence, in our intensity calculations no temperature correction was deemed necessary.

According to Bertaut (*12*), for a spinel $X^{2+}Y_2^{3+}O_4$ the value of the structure factor F may be written for a given reflection in the form:

$$F = F_0 + \lambda \Delta F_1 \qquad (2)$$

where F_o is the structure factor of the normal spinel, λ is a parameter describing the degree of inversion (λ equals zero and 0.5 for a normal and inverse spinel, respectively), Δ is the difference between the atomic scattering factor of the divalent and trivalent cations and F_1 is a numerical factor. $\lambda \Delta F_1$ is therefore the correction due to inversion. For the reflections we have selected, the values of P, F_o and F_1 (together with the classes to which the reflections belong) are given in Table III. In this Table f_X, f_Y and f_{Ox} refer to the atomic scattering factors of the divalent, trivalent and oxygen ions, respectively, and n is an integer.

For a spinel containing only two types of cation X and Y the cation distribution is conveniently described by the general formula given already in the introduction:

$$X_{1-2\lambda}\, Y_{2\lambda}[X_{2\lambda}\, Y_{2-2\lambda}]O_4. \qquad (3)$$

However, because the solid solutions contain three cations, it is not sufficient to define only one inversion parameter λ. For the spinel $Ni_xMg_{1-x}Al_2O_4$ it is convenient to characterize the cation distribution by the general formula:

$$Ni_{x\alpha}Mg_{(1-x)\beta}Al_{2\lambda}\,[Ni_{x(1-\alpha)}Mg_{(1-x)(1-\beta)}Al_{2-2\lambda}]O_4 \qquad (4)$$

where α, β, and λ are the fractions of Ni^{2+}, Mg^{2+} and Al^{3+} ions on tetrahedral sites, respectively. This amounts to the addition

TABLE III

SCATTERING FACTOR COMBINATIONS FOR THE X-RAY REFLECTIONS USEFUL IN THE DETERMINATION OF CATION DISTRIBUTION

Reflection	Class	$h^2+k^2+l^2$	P	F_0	F_1
311	b	$16n+11$	24	$f_Y + f_X/\sqrt{2}$	$-(\sqrt{2}-1)$
400	c	$16(2n+1)$	6	$2f_Y - f_X + 4f_{Ox}$	4
220	e	$16n+8$	12	f_X	-2
422	e	$16n+8$	24	f_X	-2

of only one new parameter, since from (3) and (4) it follows that

$$2\lambda = 1 - x\alpha - (1 - x)\beta. \qquad (5)$$

The intensities were computed according to Eq. (1) and Eq. (2) with the following input data incorporated in the programme:

(i) the molar composition of the spinel;
(ii) the value of a, the lattice parameter;
(iii) the value of u, the oxygen parameter;
(iv) the scattering factors for Ni^{2+}, Mg^{2+}, Al^{3+}, O^{2-} and their angular dependences;
(v) the Lorentz-polarization correction;
(vi) a dispersion correction for the nickel scattering factor.

The value of a was taken as the weighted mean of the values for $NiAl_2O_4$ and $MgAl_2O_4$, as appropriate to the composition. Thus,

$$a = xa_1 + (1 - x)a_2 \qquad (6)$$

where the suffixes 1 and 2 refer to $NiAl_2O_4$ and $MgAl_2O_4$, respectively. This approximation is justified by the almost linear variation observed (Table I). A similar weighted mean was used for u, based on the values of $u = 0.381$ and $u = 0.387$ for $NiAl_2O_4$ and $MgAl_2O_4$ respectively (*8*). International Crystallographic Tables were used for the scattering factors and Lp corrections, except that the value for the scattering factor for O^{2-} was taken from Suzuki (*15*). The atomic scattering factors of Ni were corrected for the real part of anomalous dispersion, $\Delta f' = -3.2$.

The computer programme was designed to calculate intensity ratios in 0.1 intervals of both α and β. This is equivalent to providing the intensity ratios for 100 different values of λ for each spinel. Computations were made for a total of 20 cases, namely the ratios I_{400}/I_{220}, I_{311}/I_{220}, I_{400}/I_{422}, and I_{311}/I_{422} for the spinels with $x = 0.06, 0.10, 0.25, 0.50$ and 1.00, respectively. The results were displayed in each case by constructing from the 100 computed values a family of curves of Intensity Ratio vs β $(0 < \beta < 1)$ with α varying in steps of 0.1 from 0 to 1. As an example, we illustrate in Fig. 1 the family of curves for I_{400}/I_{220} for the composition $x = 0.50$. The experimental

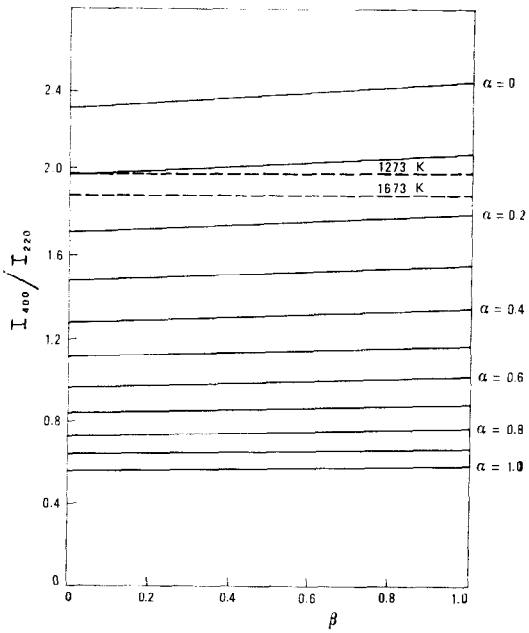

FIG. 1. X-ray diffraction intensity ratio, I_{400}/I_{220}, for different values of the inversion parameters of nickel (α) and magnesium (β) ions in $Ni_{0.5}Mg_{0.5}Al_2O_4$.

results for I_{400}/I_{220} with $Ni_{0.5}Mg_{0.5}Al_2O_4$ are shown as dashed lines in Fig. 1.

Magnetic Susceptibility

Magnetic susceptibilities were measured using an enclosed Gouy balance. The specimens with the higher nickel contents (Ni–10 and greater) were studied over the range of temperature from 98 to 290°K. In evaluating the paramagnetic susceptibility due to Ni^{2+} ions, a correction was made for the diamagnetism of the sample. The susceptibility of our $MgAl_2O_4$, measured for this purpose, was $\chi = -0.303 \times 10^{-6}$. No curvature was detectable on the plots of $1/\chi$ vs T, and only a small value was observed for the constant θ in the Curie–Weiss expression $\chi = C/(T - \theta)$. A check was made that the susceptibilities were independent of magnetic field strength. Less attention was paid to the magnetic properties of the nickel-dilute specimens (Ni–1, Ni–3 and Ni–6) on account of the larger errors incurred in dealing with such weakly paramagnetic material. A single

measurement of susceptibility at 290°K was made in these cases.

Reflectance Spectra

Reflectance spectra in the range 350–2000 nm (28,500–5000 cm^{-1}) were taken with a Beckman DK-1A spectrophotometer fitted with a reflectance attachment. $MgAl_2O_4$ served as standard for comparison.

Results

Lattice Parameters

The lattice parameter a of the cubic unit cell of each of the spinels studied is given in Table I.

There is a decrease in lattice parameter with increasing nickel content. The values of a for the specimens quenched from 1673°K are significantly higher than those of the corresponding specimens quenched from 1273°K. The variation of a with nickel fraction x is almost linear; the extents, Δa, to which the points for solid solutions are different from the ideal values corresponding to Vegard's law are reported in Table I.

X-ray Diffraction Intensities

In principle the comparison of the experimental and calculated results for two different intensity ratios is sufficient to determine both α and β, and thus the ion distribution is uniquely determined. For many spinel solid solutions this would be true in practice. In $Ni_xMg_{1-x}Al_2O_4$, however, two of the cations (Mg^{2+} and Al^{3+}) have such similar scattering factors that the exchange of them between tetrahedral and octahedral sites (α constant, β varying $0 \rightarrow 1$) produces very little change in intensity ratio (see Fig. 1). The difficulties of solving the cation distribution in $MgAl_2O_4$ by X-ray methods has long been recognised (*1*). The situation is well illustrated by Fig. 2 in which the available field of α and β values for I_{400}/I_{220} is represented for the whole range of solid solutions. The convergence of the field towards the $MgAl_2O_4$ axis ($x = 0$) illustrates the precision necessary in both calculation and experiment to obtain definitive information about β in this particular solid solution. The experimental results from Table II for the set of 1273°K-quenched specimens are entered in Fig. 2. They not only fall entirely within the

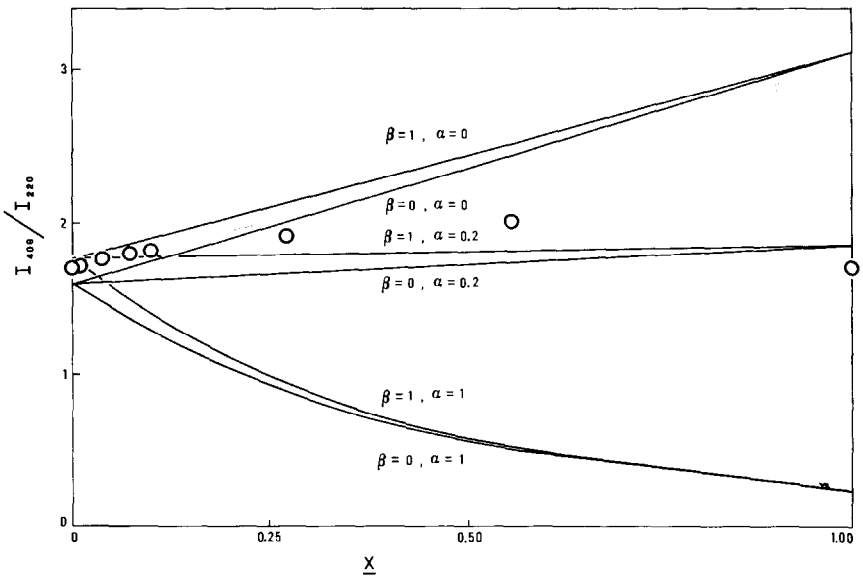

FIG. 2. Calculated X-ray diffraction intensity ratio for I_{400}/I_{220} as a function of composition (x) and of inversion parameters (α and β) for $Ni_xMg_{1-x}Al_2O_4$ solid solutions.
○ Experimental values of 1273°K-quenched specimens.

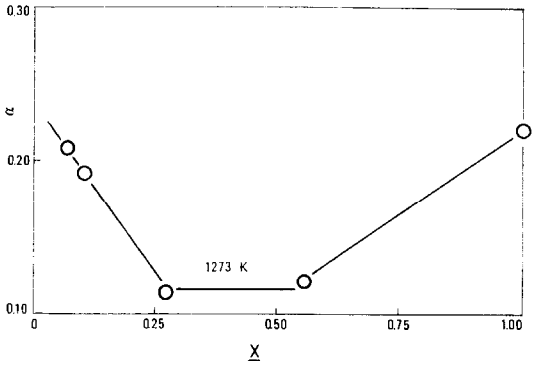

FIG. 3. Nickel inversion parameter (α) vs nickel fraction (x) in $Ni_xMg_{1-x}Al_2O_4$ quenched from 1273°K.

calculated field, but the fact that the points define such a well-developed *maximum* shows that α cannot be constant across the range $x = 0$ to $x = 1.0$, whatever the value of β. Moreover, the data imply that β is much more nearly equal to *unity* than to zero; in fact for $\beta = 0$ all the experimental points below $x = 0.25$ would fall outside the calculated field. Using plots of the type of Fig. 1, Table IV shows the results for α of our comparisons between observed and calculated intensity ratios (I_{400}/I_{220} and I_{311}/I_{220}) for the assumed case of $\beta = 1$. The mean values of α from Table IV and for the set of 1273°K-quenched specimens are shown graphically in Fig. 3. The errors on the mean α, evaluated on the basis of those derived from both the experimental and calculated intensities (*16*), are estimated at ~10%.

The results from the comparisons with both I_{400}/I_{220} and I_{311}/I_{220} are in good agreement, and the main conclusions which can be drawn from them are as follows.

(i) Ni^{2+} ions are primarily occupying octahedral sites, but there is some tetrahedral nickel in all specimens.
(ii) For a given nickel concentration in the solid solution, there is more nickel on octahedral sites in the case of samples quenched from 1273°K if β is assumed constant.
(iii) The fraction of Mg^{2+} ions in tetrahedral sites is much more nearly equal to unity than to zero.
(iv) Within each series at different temperatures, there is a minimum in α at about $x = 0.25$–0.50, if β is assumed constant in all the solid solutions.

The ratios involving the (422) reflection (Table II) are of less quantitative value than the others. Because of the relatively weak intensity, (422) in $Ni_xMg_{1-x}Al_2O_4$ does not adequately fulfil the third requirement listed by Bertaut (see above), and, being weak, it is also measured with less accuracy. Secondly, because it occurs at relatively high angle, there are increased errors in the theoretical calculation

TABLE IV

THE INVERSION PARAMETER FOR Ni^{2+} IN $Ni_xMg_{1-x}Al_2O_4$ SOLID SOLUTIONS[a]

		From I_{400}/I_{220} α (for $\beta = 1$)	From I_{311}/I_{220} α (for $\beta = 1$)	Mean α (for $\beta = 1$)
Specimens quenched from 1673°K	Ni–6	0.23	0.24	0.24
	Ni–10	0.18	0.26	0.22
	Ni–25	0.15	0.12	0.14
	Ni–50	0.17	0.12	0.15
	Ni–100	0.22	0.20	0.21
Specimens quenched from 1273°K	Ni–6	0.18	0.26	0.22
	Ni–10	0.17	0.21	0.19
	Ni–25	0.14	0.07	0.11
	Ni–50	0.13	0.10	0.12
	Ni–100	0.22	0.22	0.22

[a] α = fraction of Ni^{2+} on tetrahedral sites; β = fraction of Mg^{2+} on tetrahedral sites.

of its intensity, due to the greater uncertainty in the atomic scattering factors and their angular dependences. These drawbacks more than offset the advantage accruing from the strong dependence of (422) on the inversion parameter. The *trend* of the (422) data nevertheless matches that of the corresponding data involving the (220) reflection, which belongs to the same class (Table III), and thus affords added confirmation to our conclusions about the variations of α with x.

Magnetic Susceptibility

Although magnetic studies are less satisfactory than X-ray analysis for *absolute* measurements of nickel distribution on account of the uncertainty in the exact magnitude of the crystal field and spin-orbit coupling contribution to the magnetic susceptibility, there is the compensating advantage that the interpretation is quite unaffected by uncertainties in the magnesium distribution, no other ion in the solid solution besides nickel being paramagnetic.

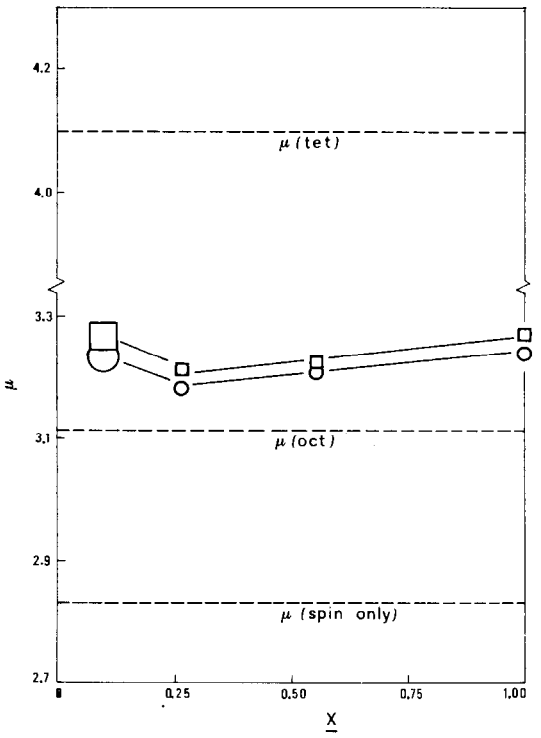

FIG. 4. Magnetic moments μ (in μ_B) of Ni^{2+} in $Ni_xMg_{1-x}Al_2O_4$ solid solutions; ○ Experimental values of 1273°K-quenched specimens, □ Experimental values of 1673°K-quenched specimens.

The results of the magnetic measurements are presented in Table I and in Fig. 4, where the theoretical values of μ for Ni^{2+} in octahedral and tetrahedral coordination are also shown. The data for Ni–1, Ni–3 and Ni–6 are very approximate, owing to the low nickel content, and are of limited value. The complete set of results nevertheless serves to show that the magnetic moments are all in the range to be anticipated for a nickel distribution which is predominantly octahedral. If we take into account the more accurate of the data (Ni–10 to Ni–100), it can be seen that there is some evidence for a minimum moment at Ni–25 (maximum of octahedral occupation). This trend in the 1673°K-quenched specimens is independently confirmed by the results on the separate set of specimens quenched from 1273°K. Furthermore, there is a consistently higher magnetic moment for the specimens quenched from 1673°K than for those quenched from 1273°K (increased tetrahedral nickel with increasing quenching temperature). Thus there is a very close parallel between the magnetic results and the X-ray results.

From the intercept on the plot of $1/\chi$ vs T, the Weiss constant θ was found to be around –20° for all specimens.

Reflectance Spectra

Reflectance spectra are a very convenient means of detecting octahedrally and tetrahedrally-coordinated nickel ions in solids. We observed 4 bands in the region 5000–28,500 cm^{-1}, some of which were only discernible as shoulders. Our spectra accorded very closely with those of Schmitz-Du Mont et al. (*17*) and with nickel aluminate spectra published by Stone and Tilley (*18*). The respective band positions for Ni–10, for example, were as follows (results of Schmitz-Du Mont et al. (*17*) in parentheses): (i) 8900 (8900), (ii) 10,000 (9800), (iii) 15,800 (15,800), (iv) 17,000 (16,800), (v) 18,200 (18,300), (vi) 23,200, and (vii) 27,000 (26,900) cm^{-1}. As pointed out by Schmitz-Du Mont et al. (*17*), band (i) is the $^3T_1$–$^3A_2$ transition of tetrahedrally-coordi-

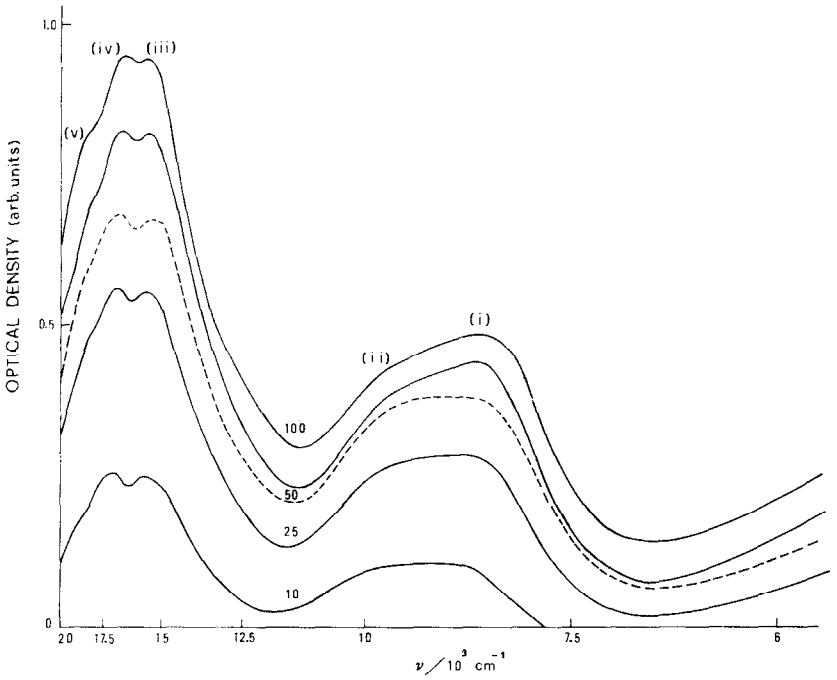

FIG. 5. Reflectance spectra of $Ni_xMg_{1-x}Al_2O_4$ solid solutions; ——Quenched from 1673°K, ---- Ni–50 specimen quenched from 1273°K. Numbers indicate nominal nickel content.

nated nickel. Band (v) is also to be associated with tetrahedral nickel, as it occurs in $Ni_xZn_{1-x}O$. Bands (ii) and (vii) are respectively the $^3A_{2g}$–$^3T_{2g}$ and $^3A_{2g}$–$^3T_{1g}$ (^3P) transitions of octahedral nickel. Bands (iii), (iv) and (vi) cannot be uniquely attributed, but are predominantly tetrahedral. Bands (i), (ii), (iii), (iv) and (v) are shown in Fig. 5 for Ni–10, Ni–25, Ni–50 and Ni–100. Bands (i), (ii), (iii), (iv), and (vii) were observed in all our specimens, and bands (v) and (vi), which are weak, were observed in all cases except Ni–1, Ni–3 and Ni–6. The results confirm conclusively that both tetrahedral and octahedral nickel are present in *all* our specimens. The tetrahedral bands dominate the spectra, but this is due to the less forbidden character of tetrahedral absorption relative to octahedral absorption, and does not signify a preponderance of tetrahedral nickel.

The bands moved to lower energies with increasing nickel content in the composition range Ni–10 to Ni–100. Figure 5, restricted to the most diagnostic part of the spectrum in order to enlarge the scale, shows this behaviour. The effect was small, amounting to 3% or less, and both octahedral and tetrahedral bands exhibited similar shift. Inspection of the relative intensities of tetrahedral and octahedral bands as a function of nickel content revealed no consistent variations. With increasing nickel content the tetrahedral bands increased more rapidly than the octahedral bands. This is simply due to their greater intrinsic absorption intensity. The effect is sufficient to mask any subtle differences due to changes in the inversion parameter with increasing nickel content. In contrast to this, the effect of temperature on inversion is easily observed, since in this case the comparison of band intensities can be made at constant nickel content. It was found that a rise in the quenching temperature from 1273 to 1673°K increased the tetrahedral absorption relative to the octahedral absorption. The effect is most readily seen in the region 7000–12,000 cm^{-1}, where tetrahedral band (i) is conveniently adjacent to octahedral band (ii).

The comparison for Ni–50 is illustrated in Fig. 5, and all other compositions showed a similar behaviour. Since the relative absorption intensity per Ni^{2+} ion in octahedral and tetrahedral sites is not precisely known, quantitative information about the magnitude of α cannot be obtained; however, it is clear that, at least 1273°K, α must be less than the random value of 0.33 in order to account for the direction of the change observed. This effect of temperature on inversion had already been observed by Schmitz-Du Mont et al. (*17*).

Comparing the band energies in spinel as a solvent with those for nickel ions in $Ni_xMg_{1-x}O$ and $Ni_xZn_{1-x}O$, we confirm with Schmitz-Du Mont et al. that both the octahedral and tetrahedral bands move to higher energies in the spinel. Expressing the effect as an energy ratio ($\bar{\nu}_{spinel}/\bar{\nu}_{MgO}$ and $\bar{\nu}_{spinel}/\bar{\nu}_{ZnO}$, respectively), we found a mean value of 1.14 for the octahedral bands and 1.04 for the tetrahedral bands. The effect is due to the coordination polyhedra being more compact in the spinel, thereby increasing Dq, the strength of the crystal field. The effect is much greater on the octahedron than on the tetrahedron.

Discussion

The distribution of cations in the spinel structure is influenced by various energy terms, such as the Madelung energy, the Born repulsive energy, the individual site-preference energy and anion polarization. For $NiAl_2O_4$ the octahedral site-preference energy makes a significant contribution to the total lattice energy and this accounts (*7*) for the highly inverse character of this spinel (78% inverse) as compared with other aluminium spinels. In the absence of site-preference energy, the Madelung energy and anion polarization terms favour the normal distribution (*8*). In "normal" aluminium spinels with small Al^{3+} ions in octahedral sites the radius ratio ($Al^{3+}/O^{2-} = 0.39$) is such that that there is anion–anion contact with a high repulsion term; thus unit cells are larger for "normal" spinels than for "inverse" spinels (*5*). $MgAl_2O_4$ is a case where there is no site-preference energy to contribute to the lattice energy: accordingly it will be a more normal spinel than $NiAl_2O_4$ and, although the radii of Mg^{2+} and Ni^{2+} are so close to one another, $MgAl_2O_4$ has a larger unit cell than $NiAl_2O_4$ (Table I). For a solid solution series of spinels, such as $Ni_xMg_{1-x}Al_2O_4$, deviations from Vegard's law can be interpreted as reflecting the variation of the cation distribution with x. The deviations, however, have to be substantial, e.g., $LiCr_xFe_{2.5-x}O_4$ (*19*), before one may use this method with confidence.

Another method to look for changes in the distribution of paramagnetic ions, such as Ni^{2+}, between octahedral and tetrahedral sites is magnetic susceptibility since there is a much greater contribution of spin-orbit coupling to the magnetic moment of Ni^{2+} in a tetrahedral field than in an octahedral field. In fact for Ni^{2+} in octahedral field (ground state $^3A_{2g}$) $\mu_{eff} = (1-4\lambda/10Dq)\mu_{s.o.}$, where λ is the spin-orbit coupling constant, Dq is the crystal field strength and $\mu_{s.o.}$ is the spin-only value of the magnetic moment (2.83 μ_B) (*20*). From the values of Dq and λ given in the literature (980 cm^{-1} and -245 cm^{-1}, respectively) (*17*, *21*), we can derive a value of 3.11 μ_B for the magnetic moment of octahedral Ni^{2+} in the $Ni_xMg_{1-x}Al_2O_4$ spinel series. The ground state of Ni^{2+} in a tetrahedral field is, instead, an orbital triplet $^3T_1$ (^3F) and its magnetic moment is accordingly appreciably increased by the orbital contribution. Experiment has shown that $\mu = 4.08$ μ_B in the spinel phase of $NiRh_2O_4$ (*8*), which has Ni^{2+} only on tetrahedral sites and $\mu = 4.1$ μ_B in the tetrahedrally coordinated $Ni_xZn_{1-x}O$ (*22*). Spin-orbit coupling will not cause the moment in ZnO to differ much from that in $MgAl_2O_4$, and in any case Dq is similar ($\bar{\nu}_{spinel}/\bar{\nu}_{ZnO} = 1.04$), so we may assume $\mu = 4.1$ for tetrahedral nickel in $MgAl_2O_4$. An increase in the magnetic moments will then indicate in the $Ni_xMg_{1-x}Al_2O_4$ spinel series an increase in Ni^{2+} tetrahedral occupation.

The other methods, namely intensity variations of some X-ray reflections and reflectance spectra, which also give information on the cation distribution, have already been described in some detail earlier in the paper.

The reflectance measurements (Fig. 5), the magnetic moments (Fig. 4) and the X-ray

diffraction intensities (Table IV) show a definite trend towards less inversion of Ni^{2+} with increasing temperature. The lattice parameters (Table I) are higher in the 1673°K quenched specimens, which agrees with the above conclusion since the lattice parameter of a spinel will increase with increasing quenching temperature (at constant composition) if the spinel *as a whole* becomes less inverted. Schmalzried (*4*), Datta and Roy (*3*) and Schmitz-Du Mont et al. (*17*) have already demonstrated that in all nickel–magnesium spinels studied by them there is an increased tendency of Ni^{2+} ions to move to tetrahedral sites with increase in temperature. The observed effect is to be expected for any spinel in which the enthalpy difference between normal and inverted states of a component ion is small and which, at low temperatures, is predominantly inverted in that species. The interchange enthalpy for the equilibrium $X^{2+}_{tet} + Y^{3+}_{oct} \rightleftharpoons X^{2+}_{oct} + Y^{3+}_{tet}$ in $NiAl_2O_4$ is only about −8.368 kJ $mole^{-1}$ (*23*).

The analyses of diffraction intensity and magnetic susceptibility (Figs. 3 and 4, respectively), show that the distribution of nickel ions between octahedral and tetrahedral sites of the spinel structure depends on nickel concentration. Our work shows conclusively that the nickel inversion parameter α is lower in Ni–25 and Ni–50 than in Ni–100 and in the nickel-dilute solid solutions ($x \to 0$). The X-ray results would be consistent with α decreasing progressively to zero as x is decreased across the range $x = 1$ to $x = 0$ if $\beta \leqslant 0.7$, but this extreme conclusion ($\alpha \to 0$ and $\beta < 0.7$) is emphatically ruled out by the fact that tetrahedral nickel has been proved to exist in Ni–6, Ni–3 and Ni–1 by reflectance.

To account for tetrahedral nickel in Ni–6 sufficient to show up in reflectance, we must postulate that β is significantly greater than 0.7. For $0.7 < \beta < 1.0$, the data require a minimum to develop in the variation of α with x. It should not be a serious approximation to infer that the β value for $MgAl_2O_4$ is appropriate also to the magnesium-rich solid solutions. $MgAl_2O_4$ used to be widely regarded as a normal spinel ($\beta = 1$), both on theoretical grounds and on the basis of neutron diffraction analysis (*24*). More recently, however, NMR (*25*) and infrared spectroscopy (*26*) have been applied to this problem, and the results from both techniques have pointed decisively to a partly inverted distribution. Reexamination by neutron diffraction has confirmed that $MgAl_2O_4$ is partly inverse (*27*) and the fraction of Mg^{2+} ions on octahedral sites has been estimated as 10–15%. This very interesting result provides us with a value of $\beta = 0.85$–0.90, which places the solution for α just inside the range where a minimum can be present and at the same time is consistent with our seeing tetrahedral nickel by reflectance in all the specimens.

Let us now consider why the octahedral occupation by nickel should reach a maximum value around $x = 0.25$. Granted that $NiAl_2O_4$ is as inverse as it is because of octahedral nickel being stabilized by the surrounding O^{2-} ion field, it is surprising at first sight that the fraction of nickel in octahedral sites at an intermediate composition in $Ni_xMg_{1-x}Al_2O_4$ (where the lattice parameter is larger than in Ni–100) should be more than in $NiAl_2O_4$. Our reflectance spectra, however, provide the clue to this anomaly. They show that *Dq* does not decrease between Ni–100 and Ni–25 but, on the contrary, the bands move to *higher* energies in Ni–25. Thus the preference energy for Ni^{2+} in octahedral sites is greater at Ni–25 than at Ni–100. There is a second important consideration. The oxygen parameter u is 0.381 in $NiAl_2O_4$ (*10*), but increases to 0.387 in $MgAl_2O_4$ (*27*). This change means that the octahedral sites in $MgAl_2O_4$ (and presumably in Ni–25) are smaller than in $NiAl_2O_4$. This is a clear proof that a factor operating to increase octahedral stabilization of nickel is at work as $NiAl_2O_4$ is diluted with Mg^{2+} ions. The result is a decrease in α as x changes from 1.0 to 0.25. We have very little knowledge about the extent to which molecular orbital formation is contributing to octahedral stabilization in this system. Blasse (*8*) has pointed out that anion polarization is greater in normal spinels than in inverse spinels and that ligand field effects may then contribute to octahedral stabilization of transition metal ions. Assuming $\alpha \sim 0.1$ and $\beta \sim 0.9$, Ni–25 is approximately 70% normal (Eq. (5)), so there may indeed be a favourable factor from this source.

On the other hand, as x decreases, the spinel as a whole becomes more normal. The electrostatic energy is the primary source of the crystal energy in spinels, and the Madelung constant is higher for a normal spinel than for an inverse one (for $u > 0.380$) (*8*). In the present case, there will not only be a rise in the Madelung constant as the spinel achieves greater normality ($x \to 0$), but the effect will be accentuated near $x = 0$, because of the high u parameter of 0.387 in $MgAl_2O_4$. Thus towards $x = 0$ we propose that the Madelung energy term begins to predominate over crystal and ligand field terms in determining the nickel distribution, and thereby leads α towards the value of β. Such an effect could account for the minimum in α. Our results indicate that there is not much change in β in the nickel-dilute region. Thus so far as the *quantity* of nickel in tetrahedral sites is concerned (i.e., the product of the inversion parameter α and the mole fraction x), there is probably a continuously increasing value between $x = 0$ and $x = 1$ in all the solid solutions we have studied, irrespective of the minimum in α.

This important result found by us, i.e., the dependence of nickel octahedral occupation on composition, seems at first sight to be in contrast with the findings of Datta and Roy (*3b*) and Schmitz-Du Mont et al. (*17*) on the same $Ni_xMg_{1-x}Al_2O_4$ system. However, the elegant studies of Datta and Roy were more devoted to the variation of cation distribution with *temperature* than with composition. The constancy of nickel distribution with x was merely inferred by these authors from the constancy of one intensity ratio and from the linear variation of a with x. Our study has shown that the variation of cation distribution with composition cannot be determined very certainly by means of only one intensity ratio nor can it be reliably deduced from the small deviations from linearity observed on the lattice parameters of the $Ni_xMg_{1-x}Al_2O_4$ system. Schmitz-Du Mont et al. (*17*) have affirmed that there was no criterion from their data to suggest that the ionic distribution depends *strongly* on x. We indeed agree with these authors that this question cannot be answered on the basis of reflectance spectra. However, in the light of our results, their data give a key to explain the minimum in α. In fact from their reflectance studies it can be concluded that: (i) the most shortwave octahedral band, which is the most diagnostic for recognizing octahedral nickel, has a pronounced maximum in energy around $x = 0.1$–0.3, and (ii) a maximum value of the interelectronic repulsion Racah parameter B also occurs around $x = 0.1$–0.3. These observations point to a higher ionicity of the bonded Ni^{2+} ions in this nickel region; this implies a higher octahedral crystal field strength for the spinels at $x \sim 0.1$–0.3. Since one of the energy terms contributing to the cation distribution in spinels, the octahedral site-preference energy, is dependent on Δ_{oct} (*6*, *7*), the maximum in nickel octahedral occupation deduced by us at $x \sim 0.25$ finds an explanation also in the variation of Dq observed by Schmitz-Du Mont et al. (*17*).

A synthesis of several experimental and theoretical methods has been necessary in order to draw conclusions about the nickel inversion parameter. The individual principles which have been used are sufficiently general to be applied to other spinels in which a knowledge of the variation of inversion parameters with composition would be of theoretical interest. Many would be easier to investigate by X-rays than $Ni_xMg_{1-x}Al_2O_4$; further related work on spinels is continuing in our laboratories. There are also other structures in which the site location of cations is finely balanced between more than one coordination, including solids such as clays and zeolites which contain cations in positions extraneous to the main structure. The search for crystal and ligand field effects in such inorganic compounds deserves much more attention than it has hitherto received.

Acknowledgments

The authors acknowledge helpful discussions with Professor A. Cimino and Dr. M. Lo Jacono, and they also express thanks to Mr. G. Minelli for some of the analytical work. Finally, the authors acknowledge the support of this work by a NATO Research Grant.

References

1. T. F. W. Barth and E. Posnjak, *Z. Krist.* **82**, 325 (1932).
2. F. Machatschki, *Z. Krist.* **82**, 348 (1932).
3. (*a*) R. K. Datta and R. Roy, *J. Amer. Ceram. Soc.* **50**, 578 (1967); (*b*) R. K. Datta and R. Roy, *Amer. Mineral.* **53**, 1456 (1968).
4. H. Schmalzried, *Z. Phys. Chem.* **28**, 203 (1961).
5. E. J. W. Verwey and E. L. Heilmann, *J. Chem. Phys.* **15**, 174 (1947).
6. J. D. Dunitz and L. E. Orgel, *J. Phys. Chem. Solids* **3**, 20 (1957).
7. D. S. McClure, *J. Phys. Chem. Solids* **3**, 311 (1957).
8. G. Blasse, *Philips Res. Rept. Suppl. No. 3* (1964).
9. J. Smit, F. K. Lotgering, and R. P. van Stapele, *J. Phys. Soc. Japan* **17**, **B-1**, 268 (1962).
10. F. C. Romeijn, *Philips Res. Rept.* **8**, 321 (1953).
11. R. J. Beals and R. L. Cook, *J. Amer. Ceram. Soc.* **40**, 279 (1957).
12. E. F. Bertaut, *Compt. Rend.* **230**, 213 (1950).
13. L. Weil, E. F. Bertaut and L. Bochirol, *J. Phys. Radium* **11**, 208 (1950).
14. M. J. Buerger, "Crystal Structure Analysis," Wiley, New York (1960).
15. T. Suzuki, *Acta Cryst.* **13**, 279 (1960).
16. E. F. Bertaut, *J. Phys. Radium* **12**, 252 (1951).
17. O. Schmitz-Du Mont, A. Lulé, and D. Reinen, *Ber. Bunsenges. Phys. Chem.*, **69**, 76 (1965).
18. F. S. Stone and R. J. D. Tilley, *Proc. 5th Int. Symp. Reactivity of Solids* (Munich 1964), p. 583. Elsevier (1965).
19. E. W. Gorter, *Philips Res. Rept.* **9**, 295 (1954).
20. C. J. Ballhausen, "Introduction to Ligand Field Theory," p. 129, McGraw Hill, New York (1962).
21. W. Low, *Phys. Rev.* **109**, 247 (1958).
22. M. Lo Jacono, P. Porta, and A. Cimino, *J. Solid State Chem.* **3**, 501 (1971).
23. A. Navrotsky and O. J. Kleppa, *J. Inorg. Nucl. Chem.* **29**, 2701 (1967).
24. G. E. Bacon, *Acta Cryst.* **5**, 684 (1952).
25. E. Brun, S. Hafner, P. Hartmann, and F. Laves, *Naturwiss.* **47**, 277 (1960).
26. S. Hafner and F. Laves, *Z. Krist.* **115**, 321 (1961).
27. E. Stoll, P. Fischer, W. Halg, and G. Maier, *J. Phys.* **25**, 447 (1964).